Published in final edited form as:
Microfluid Nanofluidics. 2014 October 1; 17(4): 693–699. doi:10.1007/s10404-014-1357-3.

Nafion Film Based Micro-nanofluidic Device for Concurrent DNA Preconcentration and Separation in Free Solution

Hongjun Song, **Yi Wang***, **Charles Garson**, and **Kapil Pant**
CFD Research Corporation, Huntsville, AL 35806, U.S.A

Abstract

This paper presents a Nafion film based micro-nanofluidic device for concurrent DNA preconcentration and separation. The principle of the device is based on the combination of (a) ion concentration polarization phenomenon at the junction of the microchannel and the nanochannels in the Nafion film to form opposing electrophoretic and electroosmotic forces acting on the DNAs, and (b) end-labeled free solution electrophoresis to harness the charge-to-mass ratio for molecular differentiation. The experiments successfully demonstrated concurrent preconcentration and separation of DNA mixture in free solution within 240s, yielding concentration ratios up to 1,150X and separation resolution of 1.85. The effect of applied electric field on the concentration and separation performance was also investigated. The device can be used as a key sample preparation element in conjunction with micro- or nano-fluidic sensors for microTAS functionality.

Keywords

ion concentration polarization; end-labeled free solution electrophoresis micro-nanofluidic; DNA preconcentration; DNA separation

1 Introduction

Microfluidic and nanofluidic lab-on-a-chip (LOC) systems have been actively studied over the past decade and hold great promise for a variety of applications in biology, medicine, and chemistry (Auroux et al. 2002; Reyes et al. 2002; Whitesides 2006; Sparreboom et al. 2009; Prakash et al. 2008; Abgrall and Nguyen 2008). Particularly, ion concentration polarization (ICP), a phenomenon that occurs at the micro-nanofluidic junction, has found broad applications in biological sample preparation and analysis (Zangle et al. 2010, 2009; Wang and Han 2008; Shen et al. 2010; Plecis et al. 2005; Mani et al. 2009; Lee et al. 2008b; Lee et al. 2008a; Kim and Meyhöfer 2008; Dhopeshwarkar et al. 2005; Cheow et al. 2010). In ICP devices, the electric double layer (EDL) forms a depletion layer that excludes the molecules with the same charge as that of the nanostructure surface (exclusion-enrichment effect) (Plecis et al. 2005) from the micro-nano channel interface.

*Corresponding author: yxw@cfdrc.com, Phone: +01-256-726-4915, Fax: +01-256-726-4806.

Theoretical models of ICP in hybrid micro–nanofluidic systems have been extensively investigated and verified by comparing with experimental results (Zangle et al. 2010, 2009; Mani et al. 2009). Complex electrokinetics behaviors, such as transport of the cationic and anionic analytes and the stacking and/or focusing of biomolecules in the micro-nanofluidic system have been thoroughly described. The unique features of ICP have also been exploited for sample preconcentration to overcome challenges in detection of low abundance targets without placing a prohibitive burden on the downstream biosensing modalities. For example, Wang et al. (Wang and Han 2008) developed a nanofluidic preconcentrator for enriching the target biomolecules before the reaction, which improves both the sensitivity and the speed of detection. Kim et al. (Kim and Meyhöfer 2008) developed a novel micro-nanofluidic device for highly selective extraction and high-throughput concentration of biomolecules. By functionalizing microtubules conjugated with target biomolecules, simultaneous extraction and concentration of various proteins was successfully achieved.

However, the need for complex nanofabrication procedures that are costly, time-consuming, and susceptible to the operating and environmental variations hinders the development of advanced functionalities and integrability for micro total analysis systems (microTAS). Recently, alternative fabrication approaches to fulfill ICP, such as polymeric nanostructures (e.g., hydrogel and Nafion film) have gained considerable attention. Dhopeshwarkar et al. (Dhopeshwarkar et al. 2005) presented a simple device harnessing a hydrogel microplug for simultaneous electrokinetic concentration of DNA and fluorescein. Lee et al. (Lee et al. 2008a) reported a high-throughput protein preconcentrator using a surface patterned Nafion film and showed a concentration factor as high as ~10^4 in 5 minutes. The device was also used to increase the local concentration of low-abundance enzyme, and to improve the reaction rate and sensitivity of the assay (Lee et al. 2008b). Cheow et al. (Cheow et al. 2010) developed a multiplexed electrokinetic concentrator to enhance the sensitivity of the standard enzyme-linked immunosorbent assay (ELISA) and 65–100X enrichment was achieved in the detection limit of two cancer biomarkers. Shen et al. (Shen et al. 2010) reported a simple device for protein preconcentration by integrating a narrow Nafion strip cut from a commercial membrane into a molded PDMS microfluidic device, and a concentration factor up to 10^4 was attained within a few minutes.

Most of prior efforts primarily focused on the utilization of the ICP for biomolecules preconcentration, and the research on ICP-enabled separation of biomolecules is scarce. Meagher et al. (Meagher and Thaitrong 2012) demonstrated a device that employs photopatterned polyacrylamide membranes to preconcentrate double-stranded DNA (dsDNA) and on-chip capillary electrophoresis (CE) to separate the concentrated DNA, respectively. However, the CE requires the use of sieving matrix (e.g., gel) to overcome the free-draining properties of DNA, and is usually time consuming, low efficient, and costly.

To address these issues, end-labeled free solution electrophoresis (ELFSE) has been developed for DNA separation in free solution (Meagher et al. 2005). Compared to the matrix-based CE separation, ELFSE provides faster separation and longer read length, which is more suitable for use in microfluidic devices. The principle of ELFSE is to attach a drag-tag at one end of the DNAs in order to vary their charge-to-mass ratio for fast, efficient separation. The early theory of ELFSE was presented by Mayer et al. (Mayer et al. 1994), in

which an uncharged label is attached to the end of the target DNA molecule to increase its mass, but keep the total charge unchanged. As a result, the charge-to-mass ratio of the label-attached DNA was modified, giving rise to the separation of unattached and label-attached DNAs. Ren et al. (Ren et al. 1999) reported the separation and sequencing of single-stranded DNA (ssDNA) based on ELFSE using a natural protein (streptavidin) as a drag-tag. The first 100 bases of a DNA sequencing reaction were achieved without any sieving matrix. In addition to the natural protein tag, some engineered protein tags have also been developed for ELFSE-based DNA separation and sequencing. Meagher et al. (Meagher et al. 2008) demonstrated the first use of a non-natural, genetically engineered protein polymer drag-tag to sequence DNA fragments by ELFSE. The engineered drag-tag has an effective drag similar to streptavidin, but is able to produce significantly clearer results, i.e., sharper peaks in the electropherogram. Won et al. (Won et al. 2005) confirmed the feasibility of ELFSE-based separation and sequencing of DNA up to 233 bases by virtue of engineered protein polymers. Furthermore, comb-like, hydrophilic, and water-soluble copolymers was successfully synthesized by Haynes et al. (Haynes et al. 2005) for ELFSE-based DNA separation. Separation of ssDNA of varying lengths up to 150 bases was successfully achieved.

Similar to most of electrophoresis-based separation techniques, ELFSE on the microfluidic platform also suffers from the low sample volume and band broadening effects due to non-uniformity in channel structures, surface properties, etc. Therefore, it is imperative to develop on-chip preconcentration capability that is inherently compatible with microfluidic ELFSE to enhance the analysis performance downstream. To address the need, in this paper we present a micro-nanofluidic device to concentrate and separate DNAs based on the innovative combination of ICP and ELFSE techniques. The device relies on ICP formation at the micro-nano channel junction to exert exclusive forces on DNA molecules against electroosmotic flow (EOF) for preconcentration, and the simultaneous DNA separation is enabled by ELFSE. The development represents an original effort that combines the nanofluidic ICP and ELFSE for concurrent preconcentration and separation of DNA at low concentration.

2 Principle and Design

Figure 1 illustrates the principle and design of our Nafion film based micro-nanofluidic device. It consists of two microchannels. One channel (highlighted in red) is used to load the sample and the other one (highlighted in blue) to load the buffer. A Nafion film intersects both microchannels at the bottom to provide electric and fluidic connection. During the experiments, different voltages are applied at the reservoirs to generate the electric field. A high voltage V_1 and a low voltage V_2 is applied at inlet and outlet reservoir of the sample channel respectively. And both the inlet and outlet reservoirs of the buffer channel are grounded (V_3=V_4=0). Such voltage configuration generates tangential electroosmotic flow (EOF) pointing from right to left (indicated by the brown arrow), and continuously drives the DNA samples from the reservoir at the top right towards the Nafion-embedded junction. Due to the ICP and the associated exclusion effect acting against the EOF, the DNA sample gets accumulated and enriched upstream of the junction. At the same time, for molecules with different charge-to-mass ratios, such as DNAs with end-labeled tags, they can also be

separated along the channel due to the differences in the exclusive forces acted on them (as shown in the inset of Figure 1a). Therefore the device enables concurrent concentration and separation of different DNAs.

3 Materials and Methods

The device comprises of two complimentary layers: (1) a microfluidic channel layer made out of polydimethylsiloxane (PDMS), and (2) a Nafion film layer on a glass substrate. The fabrication procedure is summarized in Figure 2a. The microfluidic channels were fabricated in PDMS (all the microchannels is 50 μm wide and 5 μm deep) using the standard soft lithography techniques (Xia and Whitesides 1998); and the Nafion film was fabricated on the glass substrate using the microflow patterning method (Lee et al. 2008a). Briefly, the procedure is as follows: (1) A single microchannel with 100 μm width and 50 μm depth was used and a drop of liquid Nafion perfluorinated resin 20% (wt) solution (from Sigma-Aldrich, St Louis, MO, USA) was placed on an open reservoir of the channel, and allowed to enter and fill the channel based on capillary forces. (2) The liquid resin was mostly drawn out of the microchannel by negative pressure applied through the syringe tubing at the other end of the channel. In the microflow patterning process, the thickness of the membrane is mostly controlled by the amount of the applied negative pressure. (3) By removing the microchannel, only a thin layer of Nafion film remained on top of the glass slide. The glass slide with Nafion film was placed onto the hot plate at 120 °C for baking for 1 hour. To assemble the device, the PDMS layer was aligned and bonded onto the glass substrate carrying the Nafion film using plasma bonding and heated at 95 °C for 1 hour. Both the PDMS and glass surfaces were cleaned with plasma prior to the bonding. The assembled glass-PDMS chip with the enlarged view of the Nafion junction is shown in Figure 2b.

A customized 102-mer biotinylated DNA (5′-(DyLight547)-AGC AAA ATT TAC CTT GTG TTA CGC TTA GGC AAA TTT ATT TAT TTT TAC TAT GAT CTG GGC GGC GGC AAA CTA GGC CTT GGC CAC GTG AGC GAA AAA GAT GCG-(BioTEG)-3′) was synthesized by Integrated DNA Technologies (Coralville, IA, USA). The DNA sample was resuspended in a 5 mM Tris-HCl buffer solution for experimental testing. Note that the DNA allows attachment of a streptavidin molecule onto the biotin label at the 3′-end, which serves as the drag-tag to enable ELFSE for separation (see below for more details).

The experimental protocol is given as follows: (1) before experiments, the channels were treated by 1% BSA and washed again with 100 mM Tris-HCl for 5–10 minutes; (2) 5 mM Tris-HCl buffer was loaded into the reservoirs to fill the channels; (3) a high-voltage power supply (HVS-3000D, Labsmith Corp, Livermore, CA, USA) was used to apply DC between the reservoirs; (4) DNAs were loaded into the sample reservoir and driven into the channel under properly configured electric field; and (5) the DNA preconcentration and separation at the channel-Nafion film junction was observed using Nikon TE-2000E epi-fluorescence inverted microscope and the time-lapse images were recorded using a digital camera (CoolSNAP HQ2, Photometrics, Tucson, AZ, USA).

4 Results and Discussion

In this section, we will first present the results of the DNA preconcentration, and then the concurrent preconcentration and separation of the DNAs with or without the streptavidin drag-tag. Finally, results of the parametric experiments to investigate the effect of the electric field will be described.

4.1 DNA Preconcentration

The 102-mer biotinylated DNA with 25 nM initial concentration was first used to demonstrate the preconcentration functionality of our device. The voltage difference V_{diff} across the sample channel ($V_{diff} = V_1 - V_2$) is 80 V. The snapshots of the fluorescence vs. time (t =0, 30, 60, 90, 120, 150, 180 s) in Figure 3 show the continuous accumulation and enrichment of the DNA (also see Movie_1 in the supplementary information), which is further verified by the fluorescence intensity plot along the channel centerline in Figure 5a. The maximum intensity gradually increases with time and finally reaches 70 A.U. at 180 s. It is interesting to note that the exclusion zone in the microfluidic channel propagates in an outward fashion from the Nafion film interface due to the dynamic equilibration process of ICP (Zangle et al. 2010, 2009). To quantitatively characterize the device performance, the concentration ratio, defined as the ratio of the enriched DNA concentration (average along the cross-section) to the initial concentration, as a function of time is presented in Figure 5b. The concentration ratio increases from 1X to 500X within 180 s, yielding an average concentration speed of 2.78X/s.

4.2 Concurrent Concentration and Separation of DNA Mixture

Next, we demonstrate the concurrent concentration and separation of the DNA mixture. The mixture consists of two DNAs: (1) one is the biotinylated DNA without streptavidin (free DNA), and (2) the other is the DNA with streptavidin bound at its 3′ end (bound DNA) as the drag tag. The latter was formed by conjugating free DNA to streptavidin, and then was mixed with free DNA to obtain the sample. The initial concentration of bound DNA was 5 nM and that of the free DNA was 25 nM and the voltage difference V_{diff} across the sample channel is 60 V. Figure 5 illustrates the migration, concentration, and progressive separation of the DNAs in the mixture sample (also see Movie_2 in the supplementary information). As can be seen, both free DNA and bound DNA were concentrated, and then separated with continuously growing resolution. At t = 60 s, it is impossible to distinguish the two DNA bands. However at t = 120 s, concurrent concentration and separation of the two bands is clear. Note that free DNA moves away from the Nafion junction faster than the bound DNA due to the drag imposed by the large streptavidin molecule on the latter. A clear separation was observed at t=180 s and 240 s (Figure 5), where the two bands corresponding to the free DNA and bound DNA were saliently resolved.

To quantitatively characterize the performance, both the concentration ratio and the separation resolution were calculated. The separation resolution is defined based on the distance of the peaks between the bands Δd and the widths of two DNA bands W_{free} and W_{bound} (Δd, W_{free} and W_{bound} are average values along the cross-section) (Buel et al. 2001)

$$SR = \sqrt{2(\ln 2)}\Delta d/(W_{free}+W_{bound}) \quad (1)$$

Higher concentration ratio and separation resolution represent better performance. The concentration ratio for both DNAs and the separation resolution vs. time are plotted in Figure 6 (note that the two plugs cannot be differentiated for t<90 s, and hence, these results are not shown). We can see the concentration ratio for both bound DNA and free DNA increases with the time. The final concentration ratio approximately reaches 900X and 500X for the bound and free DNA at 240 s, yielding an average concentration speed 3.75 X/s and 2.08 X/s, respectively. It should be pointed out that the bound DNA has a lower initial concentration, which leads to a longer equilibration process and a higher concentration ratio. Figure 6b shows that the separation resolution increases from 0.7 to 1.45 as the time elapse increases from 90 s to 240 s, yielding a clearer distinction between the bound DNA and free DNA.

Among all the operating parameters, the electric field over the sample channel plays the most critical role, and was extensively interrogated in the present study. Three electric potential difference V_{diff} (40 V, 60 V, and 80 V) were applied across the sample channel. The initial concentration of the bound and free DNA was set at 5 nM and 7.5 nM, respectively. Figure 7a shows the concentration ratio vs. time for both DNAs, which increases with an increase in the electric field strength. This can be attributed to the stronger exclusive forces acting on the DNAs giving rise to marked ICP and stronger electrophoretic forces and electroosmotic flow, leads to stronger concentration within a short period of time. The final concentration ratio of the bound DNA after 240 s was about 980X, 1000X, and 1150X, respectively, for V_{diff} equals 40 V, 60 V and 80 V, corresponding to the average concentration speed of 4.08X/s, 4.17X/s and 4.79X/s. Similarly, the concentration ratio for the free DNA was 970X, 990X, 1100X, corresponding to the average concentration speed of 4.04X/s, 4.13X/s and 4.58X/s, respectively. We also investigated the effect of the electric field on the separation performance. Figure 7b shows that the separation resolution dramatically increased from 0.77 to 1.85 as a result of the voltage difference V_{diff} rise from 40 V to 80 V. However, it should be noted that there is an upper limit of the applied electric difference across the sample channel due to electrolysis of the buffer solution. Obvious gas bubble formation was observed around V_{diff} =200 V (data not shown).

5 Conclusions

In this paper, we presented a Nafion film-based micro-nanofluidic device for concurrent DNA preconcentration and separation. The operating principle of the device is based on ion concentration polarization (ICP) phenomenon in conjunction with opposing electrophoretic forces and electroosmotic flow acting on the DNAs at the junction of the microchannel and the Nafion film, as well as the end-labeled free solution electrophoresis (ELFSE) to vary the mass-charge ratio to effect molecular differentiation. Extensive experiments were carried out to demonstrate the functionality of the device and characterize its performance. Critical findings are summarized as follows:

1. The Nafion film-based nanofluidic device effectively concentrated 102-mer biotinylated DNA with 25 nM initial concentration. Concentration ratio of 500X was achieved in 180 s, yielding an average concentration speed of 2.78X/s.
2. The concurrent concentration and separation of biotinylated DNAs using streptavidin as the drag-tag was successfully demonstrated. Higher concentration ratio was achieved for bound DNA due to its lower initial concentration.
3. The effect of the electric field was also investigated. It reveals that subject to the practical constraints (e.g., hardware and electrolysis complication) higher electric field is desirable for attaining higher concentration ratio and better separation resolution. Concentration ratios up to 1,150X and 1,100X for bound DNA and free DNA were achieved within 240 s, yielding an average concentration speed of 4.79X/s and 4.58X/s, respectively. Separation resolution up to 1.85 was obtained.

Supplementary Material

Refer to Web version on PubMed Central for supplementary material.

Acknowledgments

This research is sponsored by NIH/NHGRI under grant number 5R44HG004290-03. We would like to thank Prof. Jongyoon Han of Electrical Engineering and Computer Science, and Biological Engineering at Massachusetts Institute of Technology for guidance on the project and Prof. James W. Schneider of Chemical Engineering at Carnegie Mellon University for help discussion about the ELFSE.

References

Abgrall P, Nguyen NT. Nanofluidic devices and their applications. Analytical chemistry. 2008; 80 (7): 2326–2341. [PubMed: 18321133]

Auroux P-A, Iossifidis D, Reyes DR, Manz A. Micro total analysis systems. 2. Analytical standard operations and applications. Analytical chemistry. 2002; 74 (12):2637–2652. [PubMed: 12090654]

Buel E, LaFountain M, Schwartz M, Walkinshaw M. Evaluation of capillary electrophoresis performance through resolution measurements. Journal of forensic sciences. 2001; 46 (2):341–345. [PubMed: 11305437]

Cheow LF, Ko SH, Kim SJ, Kang KH, Han J. Increasing the sensitivity of enzyme-linked immunosorbent assay using multiplexed electrokinetic concentrator. Analytical chemistry. 2010; 82 (8):3383–3388. [PubMed: 20307052]

Dhopeshwarkar R, Sun L, Crooks RM. Electrokinetic concentration enrichment within a microfluidic device using a hydrogel microplug. Lab on a Chip. 2005; 5 (10):1148–1154. [PubMed: 16175272]

Haynes RD, Meagher RJ, Won J-I, Bogdan FM, Barron AE. Comblike, monodisperse polypeptoid drag-tags for DNA separations by end-labeled free-solution electrophoresis (ELFSE). Bioconjugate chemistry. 2005; 16 (4):929–938. [PubMed: 16029034]

Kim T, Meyhöfer E. Nanofluidic concentration of selectively extracted biomolecule analytes by microtubules. Analytical chemistry. 2008; 80 (14):5383–5390. [PubMed: 18517222]

Lee JH, Song Y-A, Han J. Multiplexed proteomic sample preconcentration device using surface-patterned ion-selective membrane. Lab on a Chip. 2008a; 8 (4):596–601. [PubMed: 18369515]

Lee JH, Song Y-A, Tannenbaum SR, Han J. Increase of reaction rate and sensitivity of low-abundance enzyme assay using micro/nanofluidic preconcentration chip. Analytical chemistry. 2008b; 80 (9): 3198–3204. [PubMed: 18358012]

Mani A, Zangle TA, Santiago JG. On the Propagation of Concentration Polarization from Microchannel- Nanochannel Interfaces Part I: Analytical Model and Characteristic Analysis. Langmuir. 2009; 25 (6):3898–3908. [PubMed: 19275187]

Mayer P, Slater GW, Drouin G. Theory of DNA sequencing using free-solution electrophoresis of protein-DNA complexes. Analytical chemistry. 1994; 66 (10):1777–1780.

Meagher RJ, Thaitrong N. Microchip electrophoresis of DNA following preconcentration at photopatterned gel membranes. Electrophoresis. 2012; 33 (8):1236–1246. [PubMed: 22589100]

Meagher RJ, Won J-I, Coyne JA, Lin J, Barron AE. Sequencing of DNA by free-solution capillary electrophoresis using a genetically engineered protein polymer drag-tag. Analytical chemistry. 2008; 80 (8):2842–2848. [PubMed: 18318549]

Meagher RJ, Won JI, McCormick LC, Nedelcu S, Bertrand MM, Bertram JL, Drouin G, Barron AE, Slater GW. End-labeled free-solution electrophoresis of DNA. Electrophoresis. 2005; 26 (2):331–350. [PubMed: 15657881]

Plecis A, Schoch RB, Renaud P. Ionic transport phenomena in nanofluidics: Experimental and theoretical study of the exclusion-enrichment effect on a chip. Nano letters. 2005; 5 (6):1147–1155. [PubMed: 15943459]

Prakash S, Piruska A, Gatimu EN, Bohn PW, Sweedler JV, Shannon MA. Nanofluidics: systems and applications. Sensors Journal, IEEE. 2008; 8 (5):441–450.

Ren H, Karger AE, Oaks F, Menchen S, Slater GW, Drouin G. Separating DNA sequencing fragments without a sieving matrix. Electrophoresis. 1999; 20 (12):2501–2509. [PubMed: 10499343]

Reyes DR, Iossifidis D, Auroux P-A, Manz A. Micro total analysis systems. 1. Introduction, theory, and technology. Analytical chemistry. 2002; 74 (12):2623–2636. [PubMed: 12090653]

Shen M, Yang H, Sivagnanam V, Gijs MAM. Microfluidic protein preconcentrator using a microchannel-integrated Nafion strip: experiment and modeling. Analytical chemistry. 2010; 82 (24):9989–9997. [PubMed: 20964443]

Sparreboom W, Van Den Berg A, Eijkel JCT. Principles and applications of nanofluidic transport. Nature Nanotechnology. 2009; 4 (11):713–720.

Wang Y-C, Han J. Pre-binding dynamic range and sensitivity enhancement for immuno-sensors using nanofluidic preconcentrator. Lab on a Chip. 2008; 8 (3):392–394. [PubMed: 18305855]

Whitesides GM. The origins and the future of microfluidics. Nature. 2006; 442 (7101):368–373. [PubMed: 16871203]

Won J-I, Meagher RJ, Barron AE. Protein polymer drag-tags for DNA separations by end-labeled free-solution electrophoresis. Electrophoresis. 2005; 26 (11):2138–2148. [PubMed: 15880624]

Xia Y, Whitesides GM. Soft lithography. Annual review of materials science. 1998; 28 (1):153–184.

Zangle TA, Mani A, Santiago JG. On the Propagation of Concentration Polarization from Microchannel- Nanochannel Interfaces Part II: Numerical and Experimental Study. Langmuir. 2009; 25 (6):3909–3916. [PubMed: 19275188]

Zangle TA, Mani A, Santiago JG. Theory and experiments of concentration polarization and ion focusing at microchannel and nanochannel interfaces. Chemical Society Reviews. 2010; 39 (3): 1014–1035. [PubMed: 20179822]

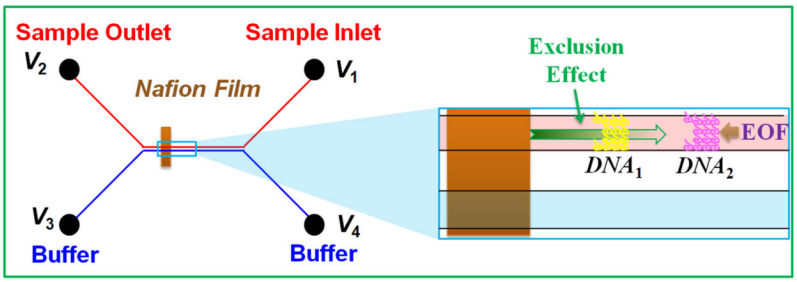

Figure 1.

Schematic of the Nafion film based micro-nanofluidic device. The sample containing end-labeled tagged DNAs is introduced from the port labeled ‘Sample Inlet’. The Nafion film is located orthogonally to the separation channel. DNAs cannot enter the nanochannels in the Nafion due to Ion Concentration Polarization (ICP) and get accumulated at the Nafion-embedded junction. The concentrated DNAs are separated by a balance of Electroosmotic Flow (EOF) and electrophoretic forces due to the differential charge-to-mass ratio generated by the end-labeled tags.

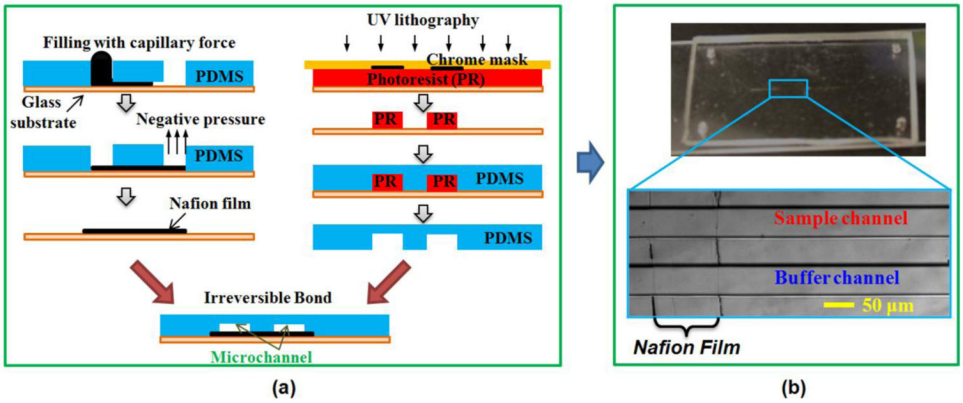

Figure 2.

(a) Microfabrication process. The fluidic channels were made out of PDMS using standard soft lithography methods. The Nafion film was fabricated using microflow patterning of Nafion resin on a glass slide, followed by curing. (b) Fabricated device. The fluidic layer was bonded to the cured Nafion-on-glass layer using plasma bonding.

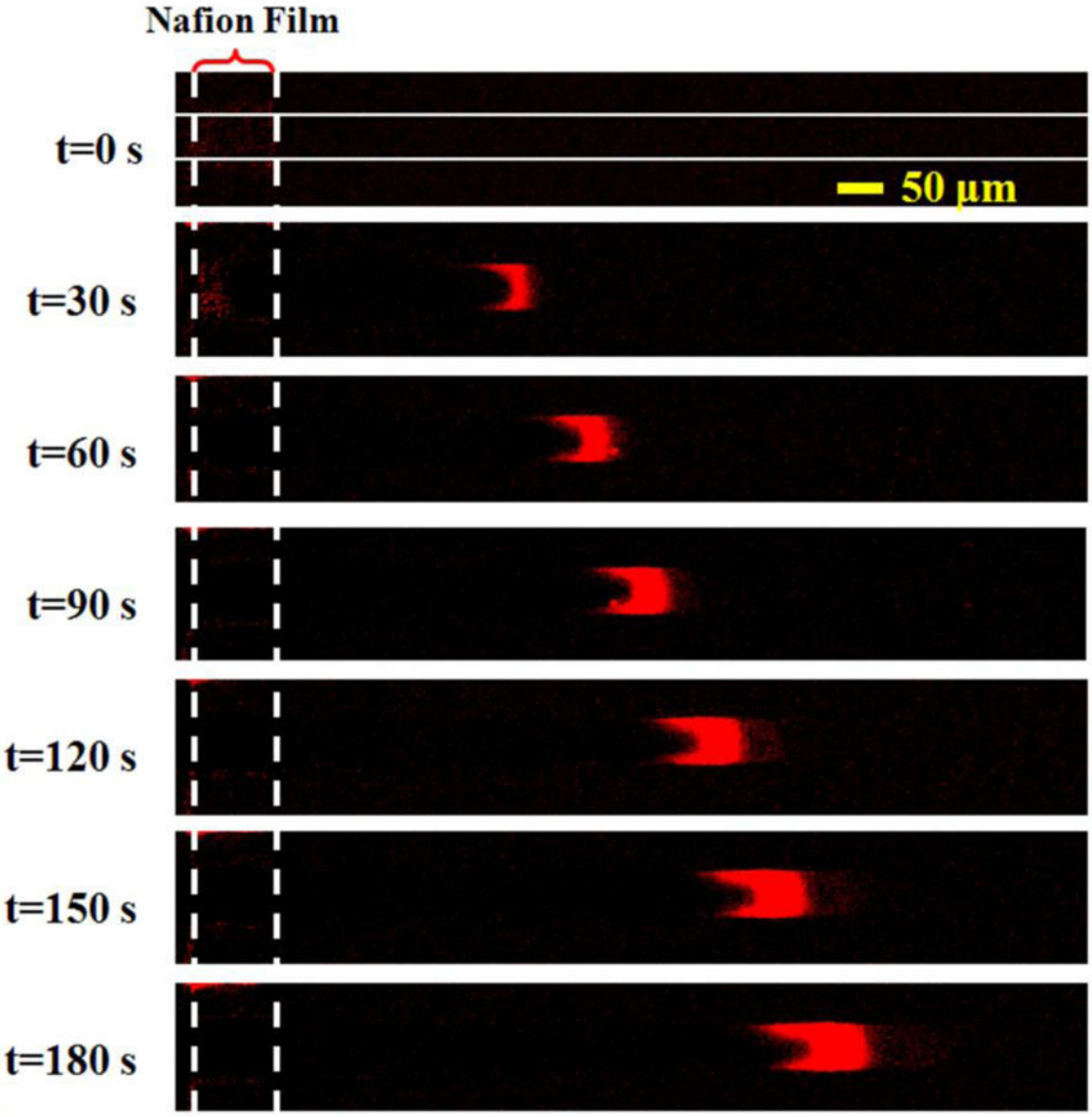

Figure 3.

Fluorescence snapshots of DNA vs. time. The fluorescence intensity increases with time, indicating concentration of the DNA sample. The exclusion zone moves away from the Nafion film interface (shown in dashed white lines) due to the dynamic equilibration process of ICP.

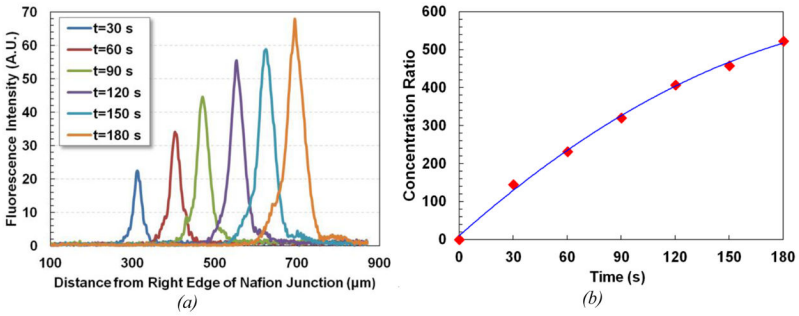

Figure 4.

(a) Fluorescence intensity along the channel centerline. The fluorescence images were post-processed to extract the intensity values at different times and are plotted as a distance from the right edge of the Nafion junction; and (b) Concentration ratio, defined as the ratio of enriched DNA concentration to the initial DNA concentration as a function of time. A concentration ratio of 500X is attained within 180 s.

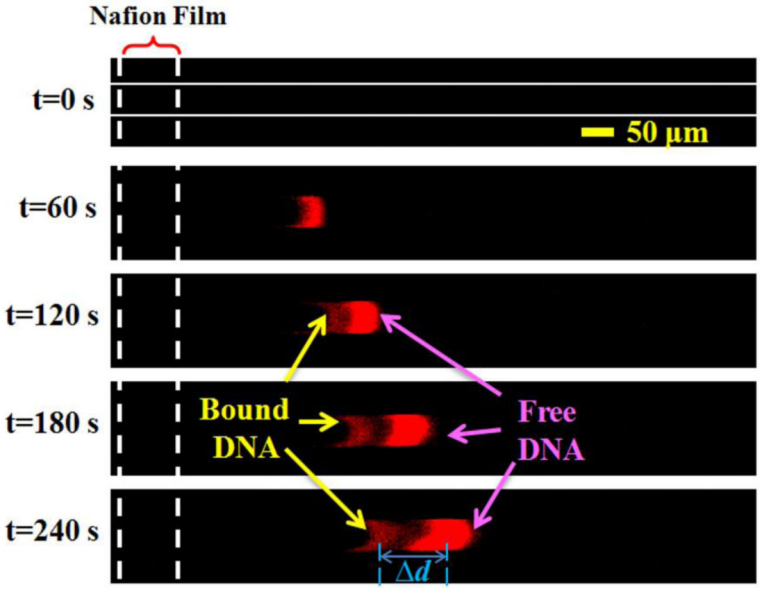

Figure 5.

Concurrent concentration and separation of the free and bound biotinylated DNAs. The free DNA consists of biotinylated 102-mer DNA whereas the bound DNA consists of streptavidin bound to the biotin end. The streptavidin acts as the drag-tag and alters the charge-to-mass ratio, leading to electrophoretic separation following DNA concentration due to ICP formation at the Nafion junction.

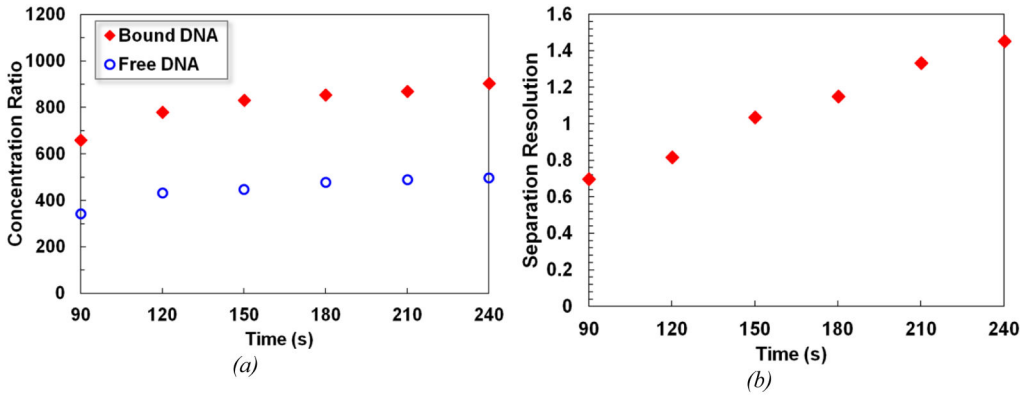

Figure 6.

(a) Concentration ratio vs. time. The peaks overlap for times < 90s (data not shown). The maximum concentration ratio bound DNA is 900X and that for free DNA is 500X. (b) Separation resolution vs. time. The separation resolution increases from ~0.7 at 90 s to reach 1.45 at 240 s.

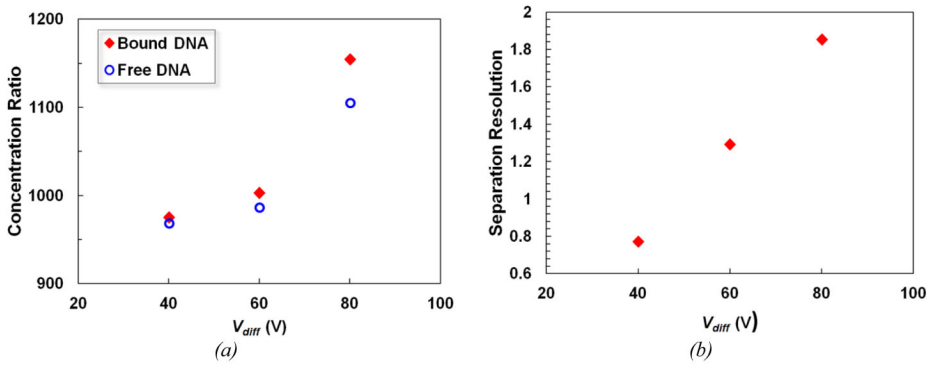

Figure 7.

Effect of electric field on (a) Concentration ratio. The concentration ratio increases almost exponentially with the applied electric field. (b) Separation resolution. The separation resolution increases linearly with the applied electric field. At higher electric fields, bubble formation was observed in the microchannels (data not shown).